

ARTICLE

GEANT4 Microdosimetry Study of Ionising Radiation Effects in Digital ASIC'sMiguel A. CORTÉS-GIRALDO^{1,*}, Francisco R. PALOMO²,
Esther GARCÍA-SÁNCHEZ² and José M. QUESADA¹¹*Departamento de Física Atómica, Molecular y Nuclear, University of Sevilla, 41080-Sevilla, Spain*²*Departamento de Ingeniería Electrónica, Escuela Superior de Ingenieros, University of Sevilla, 41092-Sevilla, Spain*

Ionisation tracks on CMOS circuits produce the so called Single Event Effects (SEE). Measuring the absorbed energy per event in the micro-structures of an integrated circuit is difficult; therefore a Monte Carlo simulation can be useful. In this work, we present GEANT4 applications to simulate the incidence of charged particles on a CMOS flip-flop designed according to AMISC5 rules. The energy per event absorbed in the flip-flop transistors is calculated for the panoply of beams available at CNA (Spanish National Accelerator Centre): proton (18 MeV) and deuteron (9 MeV) beams produced by an IBA Cyclotron, and ion beams produced by a 3-MV NEC Pelletron accelerator (9 MeV alphas, 15 MeV carbon ions and 18 MeV oxygen ions).

KEYWORDS: *GEANT4, ASIC, VLSI, microdosimetry, single event effects, heavy-ions*

I. Introduction

This work presents Monte Carlo simulations developed with the GEANT4 toolkit⁽¹⁾ (version 9.3) simulations to estimate the energy deposition in the sensitive volumes of a CMOS flip-flop by the passage of protons, deuterons and heavy-ions. The purpose of this work is to analyse and to prepare experiments at the CNA facility (Sevilla, Spain).^(2,3) Related experimental results with oxygen ions at CNA have been published recently.^(4,5)

Microelectronic devices are sensitive to the passage of ionising particles due to the nanometric scale of their components. The ionised track generates parasite charge distributions and crystalline damages, which trigger effects in the electronics leading to unexpected responses, failures and even the destruction of the device itself. These effects can be analysed and measured experimentally, and they can also be used for dosimetric measurement purposes (for example, RADFETS).⁽⁶⁾

GEANT4 has also been used for microdosimetry calculations in geometrically simple sensitive volumes of integrated RAM memories.⁽⁷⁾ In this work we also use the GDML schema to implement the complex flip-flop geometry in the GEANT4 application.⁽⁸⁾ The modelled flip-flop corresponds to a real circuit that we use in heavy-ion experiments at the CNA facility.

The energy deposited in the flip-flop, per incident particle, is calculated with the GEANT4 toolkit for several low-energy beams produced at the CNA facility. In particular, we consider the irradiation of the flip-flop by the proton (18 MeV, beam intensity of up to 100 μ A) and deuteron (9 MeV, beam intensity of up to 40 μ A) beams produced at the IBA-CNA cyclotron, and by the alpha, carbon, and oxygen beams produced at the 3-MV Pelletron accelerator at CNA. In the case of the deuteron

beam the dominant neutron stripping/knockout process in the target is not included in the simulations; therefore the neutron effects in silicon or silicon dioxide are not properly described at the present stage. That issue will be addressed in future works which will make use of the planned new capabilities for deuteron transport. GEANT4, as the other current Monte Carlo codes, such as MCNPX or PHITS, when applied for low energy deuteron transport calculations uses built-in statistical models to describe nuclear interactions. These models are found unreliable in predicting neutrons generated by low energy deuterons, mainly via direct stripping/knockout reactions. In order to overcome this limitation, an extension of the MCNPX code has been developed recently,⁽⁹⁾ which makes use of evaluated data, in much the same way as the one which is traditionally followed for low energy neutron transport. A similar development work is planned for GEANT4. At present, it is difficult to make an assertion about the effects of secondary neutrons by using GEANT4, but experimental results suggest a cross section for neutron production (deuterons on silicon at energies around 10 MeV) not less than 0.1 barn,⁽¹⁰⁾ which will presumably induce sizeable effects.

With the GEANT4 simulations we are able to calculate the energy deposition per incident particle on the flip-flop, so that an estimation of the charge collected in the sensitive volume of each CMOS transistor can be done, since the electron-hole pair production energy is well known (3.6 eV). For that purpose, it generates histograms showing the deposited energy for each sensitive volume after a pre-fixed irradiation time.

II. ASIC Geometric Model

The schematic of the flip-flop is shown at **Fig. 1**. It is a standard master-slave design, with a clock buffer input. The clock buffer has two CMOS inverter gates (4 transistors), the master stage has 4 CMOS inverter gates (14 transistors), several

*Corresponding author, E-mail: miancortes@us.es

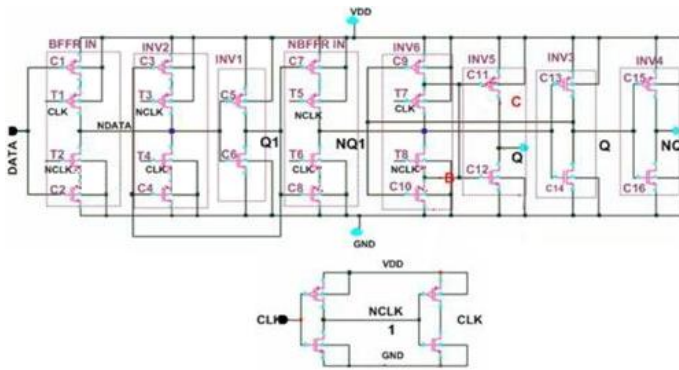


Fig. 1 Flip-Flop schematic. The flip-flop has a master-slave architecture, with an associated clock buffer.

of them with key transistors and the slave stage has 4 CMOS inverter gates (10 transistors), for a total of 28 transistors (14 nMOS and 14 pMOS). Key transistors are designated with the code TX, inverter transistors with the code CX and the clock buffer transistors with the codes nCLK nMOS, CLK nMOS, CLK pMOS and nCLK pMOS.

The flip-flop is part of a target chip used in our heavy-ion experiments. The VLSI technology kit is an On Semiconductor C5 available^a through the MOSIS programme.¹¹⁾ It is an n-well 0.5-micron, three-metal and two-polysilicon technology, very well known in the microelectronics field (it was released around mid 90's). In our flip-flop design we use only one polysilicon layer and two metal layers. The sensitive elements (drains, sources, gate oxides and channels) are under a grid of two layers of Al and a passivation layer of SiO₂ ($\approx 4 \mu\text{m}$). More details of the chip can be found elsewhere.¹²⁾

The CAD application FASTRAD¹³⁾ was used to create a precise model of the flip-flop 3D geometry (**Fig. 2**). FASTRAD creates two XML files; one describes the geometry and the other describes the materials. Both files can be used in a GEANT4 application by means of the GDML schema⁸⁾ included in the GEANT4 official release. Then, the *Detector Construction* class of our GEANT4 application uses the GDML parser to create all the physical volumes described in the XML file.

Regarding the size of the sensitive volume of each transistor, the dimensions of the drain and the source are $(x = 1.50) \times (y = 4.00) \times (z = 0.30) \mu\text{m}^3$ for pMOS elements and $(x = 1.50) \times (y = 3.00) \times (z = 0.30) \mu\text{m}^3$ for nMOS elements. The channel dimensions are $(x = 1.05) \times (y = 4.00) \times (z = 0.30) \mu\text{m}^3$ for pMOS elements and $(x = 1.05) \times (y = 4.00) \times (z = 0.30) \mu\text{m}^3$ for nMOS elements. Finally, the gate oxide (SiO₂) dimensions are $(x = 1.05) \times (y = 4.00) \times (z = 0.0125) \mu\text{m}^3$ for pMOS elements and $(x = 1.05) \times (y = 3.00) \times (z = 0.0125) \mu\text{m}^3$ for nMOS elements. The lateral dimensions of the entire flip-flop circuit are $24.0 \times 55.5 \mu\text{m}^2$. All the dimensions presented were taken from the actual layout design.

To verify the geometry, we used a GEANT4 application based on the /gdml/G01 extended example of the GEANT4

^aformerly known as AMISC5 kit from the AMS foundry.

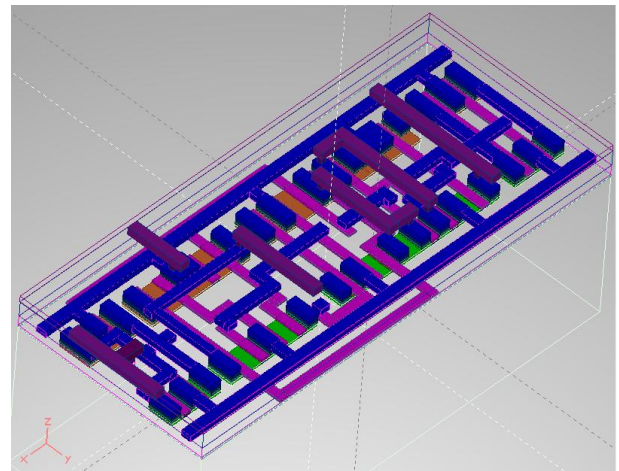


Fig. 2 Master-Slave flip-flop and clock buffer, modelled with FASTRAD for virtual irradiation with GEANT4.

toolkit. This example creates a `load_gdml` application which constructs the geometry from an XML file using the GDML schema. We modified the `vis.mac` macro in order to create a VRML file after execution. This file was read by the COSMO VRML viewer, which allowed us to verify that the geometry model created in GEANT4 with the GDML schema was reproduced properly without overlaps.

III. Irradiation Applications

In this work we have developed two applications with the GEANT4 toolkit. The aim of one application (called “ff”) is to study the energy deposition per unit volume and event in a flip-flop structure under the irradiation of beams produced at CNA facility. The other application (called “track analyser”) is devoted to calculate the linear energy deposition of particles passing through a layered geometry and to estimate the dose as a function of the radial distance to the particle track for a given incident particle, kinetic energy and target material.

These applications have been designed to track particles down to very low kinetic energies due to the nanometric scale of the flip-flop components. Thus, the so called *physics list* of these applications reproduces the electromagnetic (EM) interactions with the models implemented in the *Livermore Low-energy EM* package.¹⁴⁾ These models describe the interaction of electrons and photons with matter down to 250 eV. Cross sections are calculated by means of the evaluated data libraries EPDL97,¹⁵⁾ EEDL¹⁶⁾ and EADL,¹⁷⁾ for photons, electrons and atomic relaxations, respectively. For the rest of particles, the models provided by the *Standard-EM*¹⁸⁾ physics list have been used. For the transport of ions, we have used the GEANT4 default model of the *Standard-EM* package, which implements the effective charge approach published by Ziegler *et al.*¹⁹⁾ Hadronic interactions were simulated with a physics list based on the builder called *QGSP_BIC_HP*. In this package, the binary cascade model is implemented to simulate the hadronic interactions of protons, neutrons and ions with kinetic energy below ~ 10 GeV. Further, for neutrons with kinetic energy below 20 MeV, the *high precision* (HP) models, which imple-

ment the G4ENDL data library, are used instead of the binary cascade model.

Given the dimensions of the volumes present in the flip-flop, the *production cut* value for secondary gammas, electrons and positrons was set to an expected range of 500 nm. With this production cut, it is possible to track through the materials of the geometry (silicon, silicon dioxide and aluminium) all the secondary electrons which initial kinetic energy is greater than 250 eV. In addition, GEANT4 produces secondary electrons below this threshold if the distance between the starting point of the secondary particle and any geometric boundary is smaller than the production cut value, so that a potential bias in the results can be minimised. The energy loss due to ionisation processes which secondary electrons are not tracked is calculated by means of a continuous energy loss model.²⁰⁾ There are models under development below the range of validity of the *Livermore* models (250 eV) by the Geant4-DNA collaboration,²¹⁾ but they are intended to reproduce interactions in biological materials.

In the “ff” application, the geometry model of the flip-flop circuit is imported by means of the GDML schema. The flip-flop comprises a clock buffer, a master stage and a slave stage, described previously (Section II, Figs. 1-2). The ion beam is modelled as follows. The position of the primary particle is chosen randomly within a plane placed 10 μm above the upper surface of the flip-flop, parallel-oriented to this surface. The incidence of the primaries is perpendicular to this plane; in other words, beam aperture is considered negligible. Nevertheless, parameters of the beam such as type of particle, energy spectrum, spatial distribution and aperture of the beam can be modified via commands in a macro file. The *sensitive volumes* can be registered via interactive commands as well and scoring was performed by registering a multi-functional detector for each sensitive volume. We configured our simulations, to calculate the energy deposition per unit volume in the channel, drain, source and gate oxide of all the transistors present in the flip-flop structure.

The “track analyser” application has been designed to study the energy deposited by the passage of heavy charged particles at nanometric scale. It provides two options:

1. LET mode: The aim of the application is to calculate the linear energy deposition by heavy charged particles crossing a layered geometry. The primary particles are created at the centre of the first layer's front side with normal incidence. Each layer is divided into 0.5 μm thick sub-layers to define the *sensitive volumes* to score the energy deposited in them. Transverse dimensions are large enough to prevent all particles from crossing the walls of the geometry.
2. Radial dose mode: In this case, the aim is the estimation the energy deposition per unit volume (proportional to dose) as a function of the radial distance to the track, for a fixed incident particle, energy and material. The geometry is similar to the one described by Kobayashi *et al.*,²²⁾ which is based on an experimental setup designed by Howard Jr. *et al.*²³⁾ Our complete detection system is a cylinder with an outer radius of 1 μm and a

height of 0.1 μm . Sensitive detectors are placed within the cylinder following a “bull's-eye” structure composed of 10 nm thick concentric annular bins, ranging from an inner radius of 0 nm to an outer radius of 1 μm . Primary particles are created at the centre of the front side of the “bull's-eye” structure with normal incidence. Since the entire detection system has a thickness of 0.1 μm in the particle's direction of travel, lateral scattering can be neglected for heavy charged particles of expected range greater than $\sim 2 \mu\text{m}$. The type and kinetic energy of the incident particle and the material of the cylinders can be changed via interactive commands.

The radial dose obtained with the option 2 of the “track analyser” application are related to the linear energy deposition, which can be calculated with the option 1, by means of the formula derived by Cucinotta *et al.*,²⁴⁾

$$LET(d)_{\text{electronic}} = 2\pi \int_0^R r dr D(r, d), \quad (1)$$

where LET is the linear energy transfer of the heavy particle, d is the depth in the layered geometry, R is the maximum range of secondary electrons, r is the radial coordinate and $D(r, d)$ is the energy deposited per unit volume at a given r and d . This formula assumes that the energy deposition presents radial symmetry, which is achieved in average for a large enough number of events.

IV. Simulation Results

A total of 10^6 events were simulated with the “ff” application to calculate the energy deposited per unit volume in the drain, source and channel of each transistor of the flip-flop by 18 MeV protons (Fig. 3), 9 MeV deuterons (Fig. 4), 9 MeV alphas (Fig. 5), 15 MeV carbon ions (Fig. 6) and 18 MeV oxygen ions (Fig. 7). These values were divided by the number of events; an “event” is understood as a particle of the beam reaching the flip-flop. The error bars in Figs. 3-7 represent the statistical uncertainties (2.5%, 1σ) calculated with the method published by Walters *et al.*²⁵⁾ In these simulations, we only considered uniform irradiation on the flip-flop since the spot size of the microprobe at CNA is bigger than the flip-flop largest dimension in a factor of two, approximately. These simulations are intended to provide preliminary calculations for the experimental setup at CNA. Thus, the energy spectrum of the beam was monoenergetic. Beam aperture was neglected in the simulations, as stated previously.

The energy deposition in the elements of the flip-flop depends mainly on the surface projected normally to the beam direction and the configuration of the aluminium layers. Their geometry is not uniform throughout the flip-flop. Thus, the kinetic energy of the heavy charged particles crossing the transistor sensitive volumes depends on the total thickness of the metal layers placed above each volume. In Figs. 3-7 we observe that, for calculations with statistical uncertainties below 2.5% (1σ), the largest differences are always below the 3σ level.

Figure 8 shows the energy deposition per unit volume and event in the gate oxides of the transistors for all the beams

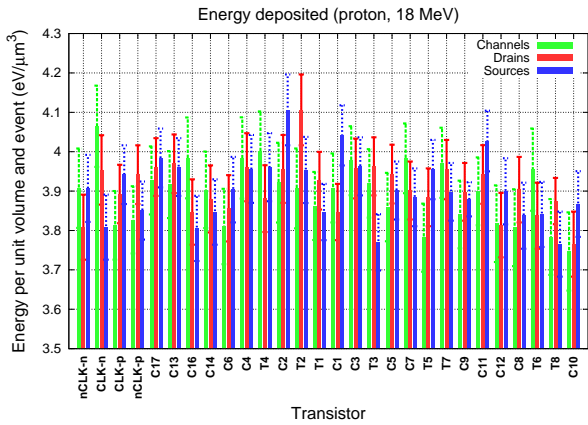


Fig. 3 Energy deposited per unit volume and event in the flip-flop elements by protons at 18 MeV. Histograms show values for channels, drains and sources. Labels in abscissa represent the corresponding transistor; in case of ambiguity, nMOS ('-n') or pMOS ('-p') type is specified.

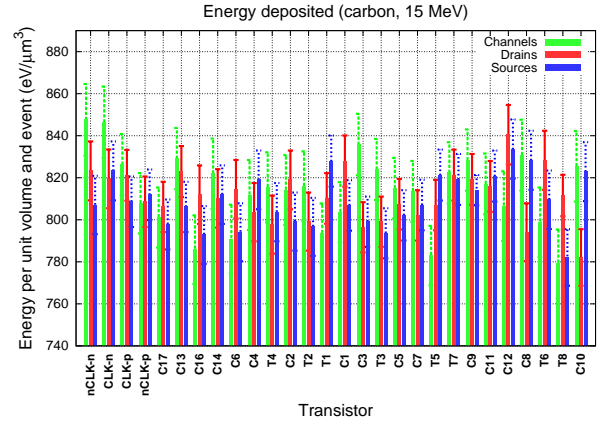


Fig. 6 Energy deposited per unit volume and event in the flip-flop elements by a carbon beam at 15 MeV. Representation criteria are the same as in Fig. 3.

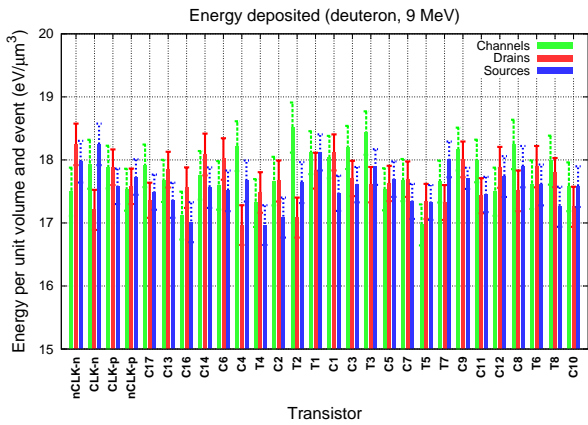


Fig. 4 Energy deposited per unit volume and event in the flip-flop elements by deuterons at 9 MeV. Representation criteria are the same as in Fig. 3.

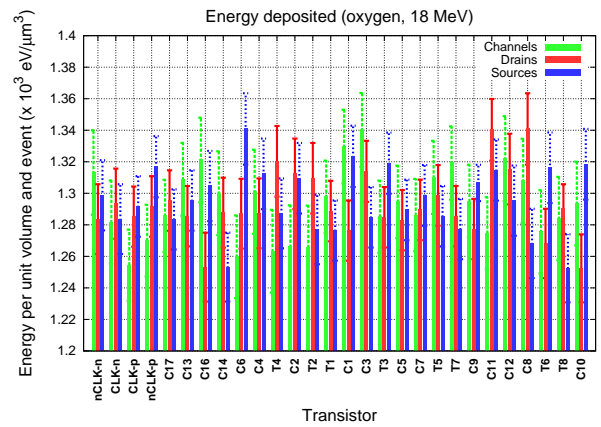


Fig. 7 Energy deposited per unit volume and event in the flip-flop elements by an oxygen beam at 18 MeV. Representation criteria are the same as in Fig. 3.

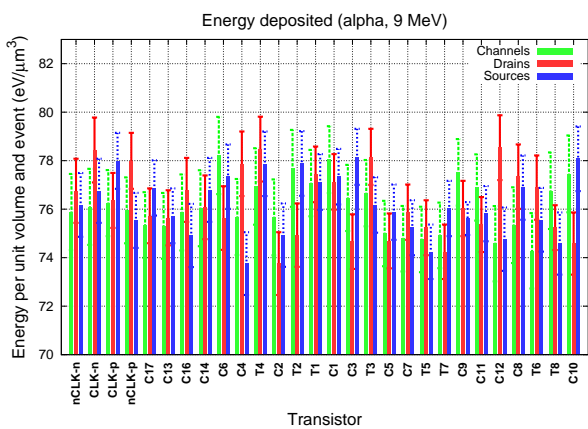


Fig. 5 Energy deposited per unit volume and event in the flip-flop elements by alphas at 9 MeV. Representation criteria are the same as in Fig. 3.

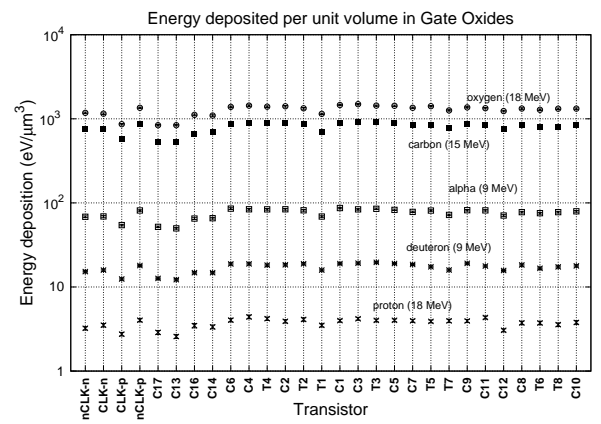


Fig. 8 Energy deposited per unit volume and event in the gate oxides of the flip-flop transistors by different beams. Symbols are larger than the error bars.

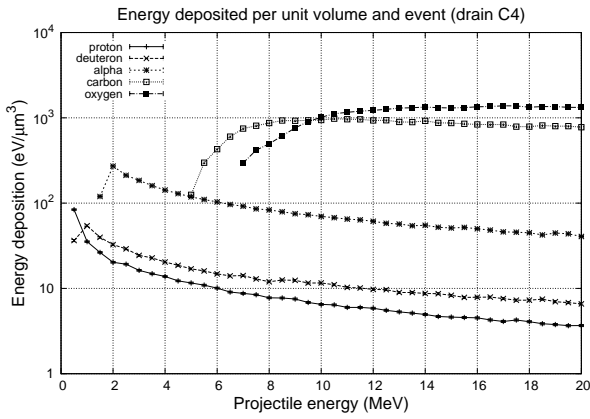


Fig. 9 Energy deposited per unit volume and event in the drain of “C4” transistor for different types of particle as a function of the beam energy.

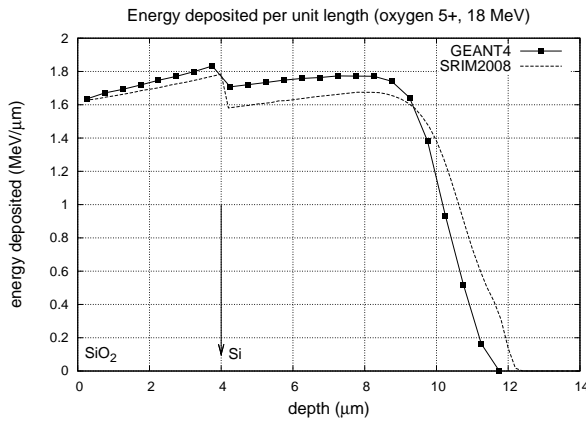


Fig. 10 Linear energy deposition of 18 MeV oxygen ions incident on a 4 μm thick SiO₂ layer followed by a 12 μm thick Si layer (bulk). The sensitive volumes of the transistors are at depths between 4-6 μm. Total linear energy transfer calculated with SRIM-2008.04 is also presented.

studied in the present work. A total of 10⁶ events were simulated and the statistical uncertainties of the calculations are below 3%. In this case, a general trend of the energy deposition can be observed. Since the gate oxides are placed at the same depth in the flip-flop, the differences found in the values presented in Fig. 8 are due to the non-uniform geometry of the flip-flop metal layers.

Figure 9 is an illustrative graph presenting the energy deposition per unit volume and event in the drain of “C4” transistor for different types and energies of the beam. As expected, the minimum beam energy needed to irradiate this volume increases with the *Z* of the ion. Also, the beam energy where the maximum energy deposition is achieved increases with the *Z* and mass of the incident particle.

Figure 10 shows the output of the “track analyser” application in the LET mode for oxygen ions entering at 18 MeV in a 4 μm thick SiO₂ layer followed by a 12 μm thick Si layer. GEANT4 results were compared to those provided by SRIM-2008.04. The energy loss models applied by GEANT4 for

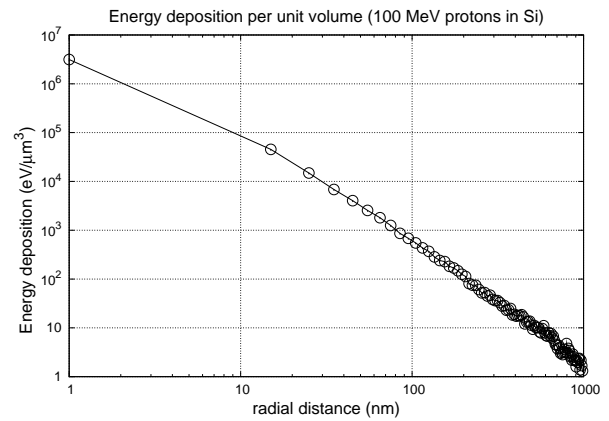


Fig. 11 Dose calculated with GEANT4 as a function of the radial distance for protons at 100 MeV in silicon. The line has been added as guide to the eye.

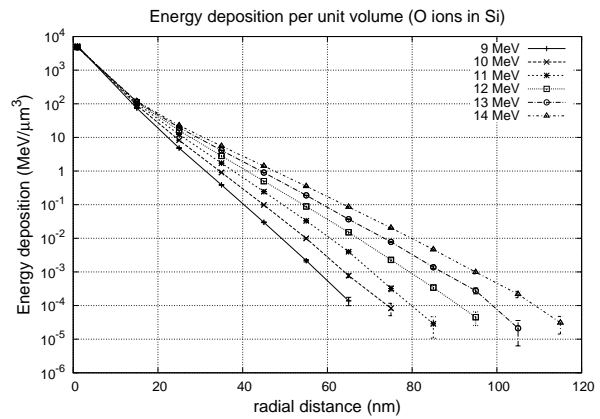


Fig. 12 Dose calculated with GEANT4 as a function of the radial distance for oxygen ions in silicon at energies ranging from 9 MeV to 14 MeV.

heavy charged particles are the Bethe-Bloch model, for kinetic energy above 2 MeV/A, and the Bragg model, which uses the parametrisation compiled in the ICRU’49 report,²⁶⁾ below 2 MeV/A.²⁰⁾ The effective charge approach developed by Ziegler *et al.*¹⁹⁾ is used, as stated previously. The agreement between both curves is within 10%, which is the precision of the GEANT4 models at this energy range.^{27)b}

Figure 11 shows the output of the “track analyser” application in the radial dose mode for 100 MeV protons incident on silicon. Each annular bin has been represented at the centre of its interval except the central bin (0-10 nm), which has been represented at 1 nm because the graph is log-log. This plot illustrates a cross-check with the results published by Kobayashi *et al.*²²⁾ In that work, the authors compared their calculations against the Katz analytical track model described by Waligorski *et al.*²⁸⁾

Figure 12 plots the radial dose distribution of oxygen ions travelling in silicon at 9-14 MeV, calculated with the radial dose mode of the “track analyser” application. The estimated value of the lateral radius of secondary electrons ranges from

^bV. Ivanchenko, private communication

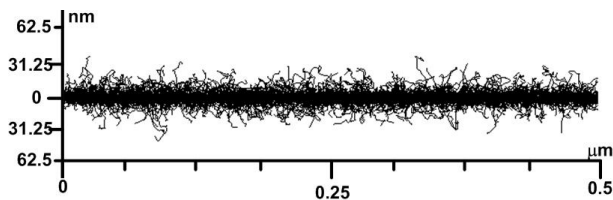


Fig. 13 Illustration of the secondary electrons produced by oxygen ions at 10.5 MeV entering in a 0.5 μm thick Si layer. A total of 10 events are reproduced. Scales are drawn for clarity reasons.

60 nm (9 MeV) to 110 nm (14 MeV). With these calculations we can estimate the lateral radius of the tracks passing through the sensitive volumes of the flip-flop. They are placed at depths between 4–6 μm , which means that 18 MeV oxygen ions reach the sensitive volumes with a kinetic energy of around 10.2 MeV. This means that the lateral radius of the track in the sensitive volumes of the transistors is around 70–80 nm.

Finally, for illustrative purposes, **Fig. 13** shows a visualisation of the accumulated tracks produced by 10.5 MeV oxygen ions in silicon, simulated with our “track analyser” application. A total of 10 events are depicted in this illustration. It can be observed that most of the secondary electrons are absorbed at radial distances lower than 20 nm. This illustration agrees with the calculations presented in Fig. 12, where the radial dose distribution falls several decades for increasing radial distance.

As it has been shown, “track analyser” calculates particle depth range, linear energy deposition (which corresponds to linear energy transfer provided that secondary particle range is smaller than the bins used in the calculation), and lateral dose range. These results can be used as inputs for the ionisation volume model in commercial simulators of electronic transport in devices under particle irradiation like, for example, Sentaurus Device TCAD²⁹⁾ or Device3D TCAD.³⁰⁾ With the ionisation volume model as input, those TCAD simulators calculate the internal electric field and expected output signals (current, voltage) produced by the device in response of the particle impact.³¹⁾

V. Conclusions

Microdosimetry Monte Carlo simulations of a realistic flip-flop under heavy-ion irradiation have been presented in this work. The simulations use two application tools coded with the GEANT4 (v9.3) toolkit. With the “ff” application we are able to estimate the energy deposition for each sensitive volume of a microelectronic device, which geometry model can be imported to GEANT4 using the GDML schema. Further, the “track analyser” application is a tool developed to analyse the energy deposition at nanometric scales. These calculations are useful to develop an ionisation volume model in the sensitive volumes for its application as input data in commercial simulators of electronic transport in devices under irradiation, like Sentaurus Device TCAD or Device3D TCAD.

Hence, these GEANT4 simulations will provide useful data to assess radiation damage of the real flip-flop under the irradiation with different beams produced at CNA (Sevilla, Spain) in future experiments.

Acknowledgments

The authors would like to thank V. Ivanchenko (CERN) for his kind help with the energy loss models implemented in GEANT4 for the transport of heavy charged particles. This work was supported by Junta de Andalucía and the Spanish Ministerio de Ciencia e Innovación Contracts P07-FQM-02894, FIS2008-04189 and FPA2008-04972-C03.

References

- 1) S. Agostinelli *et al.*, “GEANT4-A simulation toolkit,” *Nucl. Instr. Meth. Phys. Res.*, **A506**, 250-303 (2003).
- 2) J. García-López, F. J. Ager, M. Barbadillo-Rank, F. J. Madrigal, M. A. Ontalba, M. A. Respaliza, M. D. Ynsa, “CNA: The first accelerator-based IBA facility in Spain,” *Nucl. Instr. Meth. Phys. Res.*, **B163**, 1137-1142 (2000).
- 3) J. García-López, I. Ortega-Feliu, Y. Morilla, A. Ferrero, “The new Cyclone 18/9 beam transport line at the CNA (Sevilla) for high energy PIXE applications,” *Nucl. Instr. Meth. Phys. Res.*, **B266**, 1583-1586 (2008).
- 4) F. R. Palomo, Y. Morilla, J. M. Mogollón, J. García-López, J. A. Labrador, M. A. Aguirre, “Early works on the nuclear microprobe for microelectronics radiation tests at the CEICI,” *Proc. Int. Conf. on Nuclear Microprobe Technology and Applications*, Leipzig, Germany, July 26-30, 2010 (2010).
- 5) F. R. Palomo, Y. Morilla, J. M. Mogollón, J. García-López, J. A. Labrador, M. A. Aguirre, “Early works on the nuclear microprobe for microelectronics radiation tests at the CEICI,” *Nucl. Instr. Meth. Phys. Res. B*, Special issue on Int. Conf. on Nuclear Microprobe Technology and Applications, doi: 10.1016/j.nimb.2011.02.019, in press (2011).
- 6) J. Seon, S-J. Kim, B-I. Sung, S. Al Marri, S-H. Lee, “A small space radiation monitor capable of measuring multiple $I_{SD-V_{GS}}$ values of MOSFET,” *J. Nucl. Sci. Technol.*, **47**[4], 340-344 (2010).
- 7) C. Inguibert, S. Duzellier, R. Ecoffet, “Contribution of GEANT4 to the determination of sensitive volumes in case of high-integrated RAMs,” *IEEE Trans. Nucl. Sci.*, **49**[3], 1480-1485 (2002).
- 8) R. Chytracsek, J. McCormick, W. Pokorski, G. Santin, “Geometry description markup language for physics simulation and analysis applications,” *IEEE Trans. Nucl. Sci.*, **53**[5], 2892-2896 (2006).
- 9) P. Sauvan, J. Sanz, F. Ogando, “New capabilities for Monte Carlo simulation of deuteron transport and secondary products generation,” *Nucl. Instr. Meth. Phys. Res.*, **A614**, 323-330 (2010).
- 10) R. L. Wilson, D. J. Frantsvog, R. Kunselman, C. Détraz, “Excitation functions of reactions induced by 1H and 2H ions on natural Mg, Al and Si,” *Phys. Rev.*, **C13**, 976-983 (1976).
- 11) Website of MOSIS, <http://www.mosis.com>
- 12) F. R. Palomo, J. M. Mogollón, J. Nápoles, H. Guzmán-Miranda, A. Pérez Vega-Leal, M. A. Aguirre, P. Moreno, C. Méndez, J. R. Vázquez de Aldana, “Pulsed laser SEU cross section measurement using coincidence detectors,” *IEEE Trans. Nucl. Sci.*, **56**[4], 2001-2007 (2008).
- 13) Website of FASTRAD software, <http://www.fastrad.net>

- 14) S. Chauvie, S. Guatelli, V. Ivanchenko, F. Longo, F. Mantero, B. Mascialino, P. Nieminen, L. Pandola, S. Parlati, L. Peralta, M. G. Pia, M. Piergentili, P. Rodrigues, S. Saliceti, A. Trindale, "Geant4 Low Energy Electromagnetic Physics," *IEEE Nucl. Sci. Symp. 2004 Conf. Rec.*, **3**, 1881-1885 (2004).
- 15) D. E. Cullen, J. H. Hubbell, L. Kissel, *EPDL97: the Evaluated Photon Data Library, '97 version*, UCRL-50400, vol. 6, rev. 5, Lawrence Livermore National Laboratory (LLNL) (1991).
- 16) S. T. Perkins, D. E. Cullen, S. M. Seltzer, *Tables and Graphs of Electron-Interaction Cross-Sections from 10 eV to 100 GeV Derived from the LLNL Evaluated Electron Data Library (EEDL), Z=1-100*, UCRL-50400, vol. 31, Lawrence Livermore National Laboratory (LLNL) (1991).
- 17) S. T. Perkins, D. E. Cullen, M. H. Chen, J. H. Hubbell, J. Rathkopf, J. Scofield, *Tables and Graphs of Atomic Subshell and Relaxation Data Derived from the LLNL Evaluated Atomic Data Library (EADL), Z=1-100*, UCRL-50400, vol. 30, Lawrence Livermore National Laboratory (LLNL) (1991).
- 18) H. Burkhardt, V. M. Grichine, V. N. Ivanchenko, P. Gumplinger, R. P. Kokoulin, M. Maire, L. Urban, "Geant4 'standard' electromagnetic physics package," *Proc. MC2005*, Chattanooga, Tennessee, April 17-21, 2005, American Nuclear Society, LaGrange Park, IL, USA (2005), [CD-ROM].
- 19) J. F. Ziegler, J. P. Biersack, U. Littmark, *The Stopping and Ranges of Ions in Solids, Vol. 1*, Pergamon Press, 1985.
- 20) Website of the GEANT4 physics reference manual, <http://geant4.cern.ch/support/userdocuments.shtml>
- 21) S. Chauvie, Z. Francis, S. Guatelli, S. Incerti, B. Mascialino, P. Moretto, P. Nieminen, M. G. Pia, "GEANT4 physics processes for microdosimetry simulation: design foundation and implementation of the first set of models," *IEEE Trans. Nucl. Sci.*, **54**[6], 2619-2628 (2007).
- 22) A. S. Kobayashi, A. L. Sternberg, L. W. Massengill, R. D. Schrimpf, R. A. Weller, "Spatial and Temporal characteristics of Energy deposition by protons and alpha particles in silicon," *IEEE Trans. Nucl. Sci.*, **51**[6], 3312-3317 (2004).
- 23) J. W. Howard, R. C. Block, W. J. Stapor, P. T. McDonald, A. B. Knudson, H. Dassault, M. R. Pinto, "A novel approach for measuring the radial distribution of charge in heavy-ion track," *IEEE Trans. Nucl. Sci.*, **41**[6], 2077-2084 (1994).
- 24) F. A. Cucinotta, R. Katz, J. W. Wilson, "Radial distribution of electron spectra from high energy ions," *Radiat. Environ. Biophys.*, **37**[4], 259-265 (1998).
- 25) B. R. B. Walters, I. Kawrakow, D. W. O. Rogers, "History by history statistical estimators in the BEAM code system," *Med. Phys.*, **29**, 2745-2752 (2002).
- 26) ICRU (A. Allisy *et al.*), *Stopping Powers and Ranges for Protons and Alpha Particles*, ICRU Report 49 (1993).
- 27) S. Guatelli, B. Mascialino, M. G. Pia, M. Piergentili, L. Pandola, S. Parlati, K. Amako, K. Murakami, T. Sasaki, L. Urban, M. Maire, V. Ivanchenko, "Precision validation of GEANT4 electromagnetic physics," *Proc. of The Monte Carlo Method: Versatility Unbounded in a Dynamic Computing World*, Chattanooga, Tennessee, April 17-21, 2005, American Nuclear Society, LaGrange Park, IL, USA (2005), [CD-ROM].
- 28) M. P. R. Waligorski, R. N. Hamm, R. Katz, "The radial distribution of dose around the path of a heavy ion in liquid water," *Nucl. Tracks Radiat. Meas.*, **11**, 309-319 (1986).
- 29) Website of Sentaurus Device, <http://www.synopsys.com/Tools/TCAD/DeviceSimulation/Pages/SentaurusDevice.aspx>.
- 30) Website of Device3D, http://www.silvaco.com/products/vwfi/atlas/device3d/device3d_br.html.
- 31) F. R. Palomo, J. M. Mogollón, J. Nápoles, M. A. Aguirre, "Mixed-mode simulations of Bit-Flip with pulsed laser," *IEEE Trans. Nucl. Sci.*, **57**[4], 1884-1891 (2010).